Analysis of Charged Fusion Product Rates: Initial Data from the Mega Amp Spherical Tokamak (MAST)

Pierre Avila
Mentor: Werner Boeglin
Florida International University Dept. Of Physics

October 7, 2013

Abstract: Tokamaks are used to create high temperature plasmas that are studied intensively with the use of various diagnostic equipment. Charged particles such as protons and tritons emitted from fusion temperature plasmas follow complicated trajectories due to their electromagnetic interaction with the magnetic fields inside the tokamak. The objective of this study is to detect these charged particles which give a different insight to the stability of plasmas generated within the tokamak. At the Mega Amp Spherical Tokamak (MAST) located at the Culham Centre for Fusion Energy (CCFE), solid state surface barrier detectors (SSBDs) were installed inside the vacuum to detect protons and possibly tritons. The SSBDs converted the particle's energy into electrical signals, which were then amplified and recorded by a Data Acquisition system (DAQ). Protons and tritons were successfully recorded after an initial data analysis.

KEYTERMS *charged fusion products, fast ions, fusion plasmas, proton rates*

Contents

1 Introduction

1.1 Plasma Physics Background

Plasma refers to a gas where the majority of its atoms have been ionized. [1][p.1-3] Ionization is the process by which the electrons that orbit the nucleus gain enough energy to break free from the nucleus. [1][p.2] Deuterium[1] plasma is created and studied at the Mega Amp Spherical Tokamak (MAST).

The tokamak was developed in the Soviet Union during the 1960s and can create and confine plasmas. [3] The word tokamak is an acronym of a Russian description that translates into ”toroidal chamber with an axial magnetic field”. [8] Tokamaks use a variety of methods to heat and contain plasmas. First, the deuterium gas must be introduced into the vacuum vessel by means of an injection system. [3] The vessel is a toroidal chamber that is maintained at an Ultra High Vacuum (UHV), up to 10^{-10} Torr. [5] Keeping the vessel at UHV reduces the amount of impurities that are mixed into the deuterium gas when it is introduced.

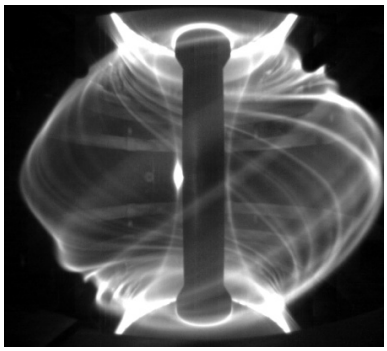

Figure 1: General Spherical Plasma Structure during a plasma shot. [6]

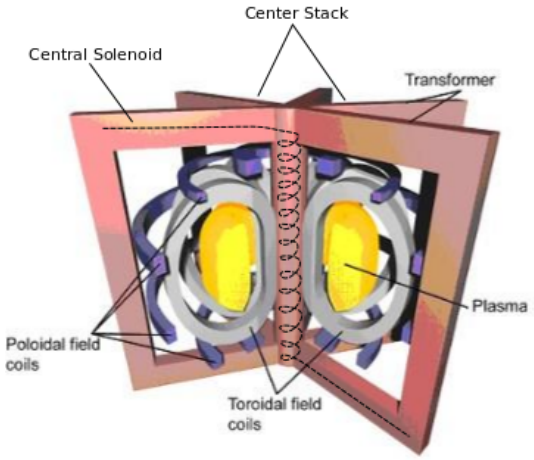

Figure 2: Tokamak Structure. [7]

Transitioning the Deuterium gas into plasma requires using various heating methods. The so called center stack is used as part of a transformer system to induce a current in the plasma (See Figure 2). [3] A time varying current is run through the central solenoid in the central stack which acts as a primary transformer winding. [3] The deuterium plasma acts as the secondary

[1]Deuterium is an isotope of hydrogen consisting of one proton and one neutron. [1][p.18]

winding in this transformer. The electric current in the plasma heats and increases its temperature, a technique known as Ohmic Heating. [3] Ohmic Heating is efficient in the early stages of the plasma creation or "plasma shot", but becomes inefficient as the plasma reaches higher temperatures. Other heating methods are introduced in order to further increase the plasma temperature. One heating method is called the Neutral Beam Injection, where a stream of energetic deuterium atoms is injected into the plasma. [3] [4] An alternative method is to use radio frequency radiation similar to microwave ovens to further heat and ionize the plasma. [3] Typical plasma temperatures are of the order of 100 million degrees centigrade. [3] [4] Nuclear fusion is the process by which two nuclei approach each other closely enough for the short range strong nuclear force to dominate and fuse the two nuclei together. Typical nuclear fusion reactions are as follows:

$$^2H +^2 H \rightarrow^1 H +^3 H + 3.27MeV$$

$$^2H +^2 H \rightarrow^3 He +^1 n + 4.03MeV$$

Figure 3: ^2H is Deuterium, ^3H is Tritium, ^1H is a proton, ^1n is a neutron and ^3He is Helium-3. [1][p.18]

Two magnetic fields are needed to confine the hot plasma, the poloidal field and the torodial field. [3] The poloidal field is produced from the plasma current and a set of coils that run parallel to the torus, while the toroidal field coils are successively wrapped around the vessel. The combination of the toroidal and poloidal magnetic fields now give rise to a helical field that contains the plasma, and is referred to as a "magnetic cage" (See Figure 4). [3] Charged particles follow the magnetic field by gyrating along the field lines, this

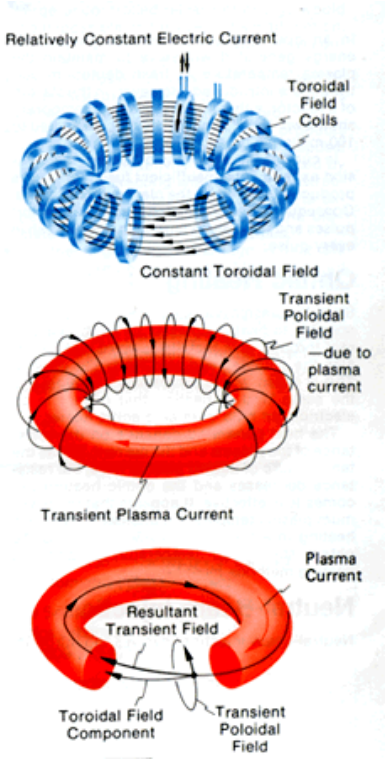

Figure 4: Magnetic Fields [9]

property combined with the magnetic field

configuration confines the plasma, keeping it from coming into contact with the vessel wall. [1][p.37-42]

1.2 Experiment Background

The Charged Fusion Product Diagnostic (CFPD) consists of four Solid State Surface Barrier Detectors (SSBDs) with collimators positioned at specific angles to detect charged nuclear reaction products emitted from a particular volume of the plasma. The CFPD is mounted at the end of a reciprocating probe arm that allows one to position the system and measure proton rates at different radial positions. The necessary orientation was determined from calculated 3 MeV proton orbits for a given detector radial position. [5] Most of the protons confined in the plasma have an energy of 1 to 2 keV. This low energy relates to a small gyro radius opposed to the protons of interest which have a much larger gyro radius.

Data received during this experiment will be compared to MAST neutron rates measured by the Fission Chamber and Neutron Camera. The Fission Chamber counts the number of neutrons emitted by the plasma that pass through the chamber. [10] The Neutron Camera uses collimators to sample neutron rates from different volumes in the plasma. [10] Detecting protons provides a new insight into nuclear fusion rates inside the plasma.

2 Experimental Methods

2.1 Data Acquisition

The protons that follow the calculated trajectories deposit themselves into the SSBDs' active area. In the sensitive area of the detector they deposit all of their energy creating a number of electron-hole pairs proportional to their energy. The signals are transported by coaxial vacuum cables to electrical feed-throughs to air side cables. Preamplifiers amplify these signals and transmit them to shaping amplifiers. By integrating and differentiating the signals appropriately, electrical noise is reduced down to a manageable level so as to make proton and triton signals discernible.

These analog signals are then digitized at a rate of 60 MHz. In essence, the digitizer saves voltage values every 16.67 nanoseconds and stores these values in files on a computer hard disk for future analysis. Each detector on the CFPD is connected to its own preamplifier, amplifier and digitizer port and each individual system is referred to as a channel. The digitizer is controlled by the Data Acquisition System (DAQ) software. Plasmas last typically for no longer than 500 milliseconds. The DAQ begins recording data shortly after the start of the plasma shot and ends several milliseconds after to ensure acquisition of the whole shot. The 500 milliseconds of plasma activity, approximately 23 MB of data per channel, is the primary range of interest. [5]

Preliminary testing of the DAQ utilized an oscilloscope that displayed voltage as a function of time and revealed a high amount of electrical noise. Fast and high frequency noise at around 500 millivolts drowns out protons and triton voltage signals. Altering the signal's amplification did not rectify the electrical noise. To be able to detect the small proton signals, several ground/earth connections were constructed to lower the electrical noise level. A sufficient drop to 100 millivolts in electrical noise was achieved making proton detection possible.

2.2 Data Analysis

In order to identify proton signals, the signal voltage as a function of time is studied. The primary objective is to identify proton signals above the electrical noise. Good proton identification is necessary to extract proton rates for the various detector radial positions relative to the tokamak center. The Python program "wx_digiplot" is used to analyze the data, namely to find peaks, histogram peak heights and to count the number of proton events occurring during regular time intervals (time slices). A peak is evidence of the detection of a charged particle, see Figure (5). The "Peak Finding Script" analyzes each point and returns a list of peak's respective voltage and time. A separate criterion implemented, the threshold, only allows peaks above a certain minimal voltage value and is entered by the user. The basis for determining the threshold is dependent on the minimum voltage value that catalogs the maximum number of proton and triton peaks excluding as much noise as possible.

The peak finding algorithm (See Section 2.3) reads voltage values and consecutively checks

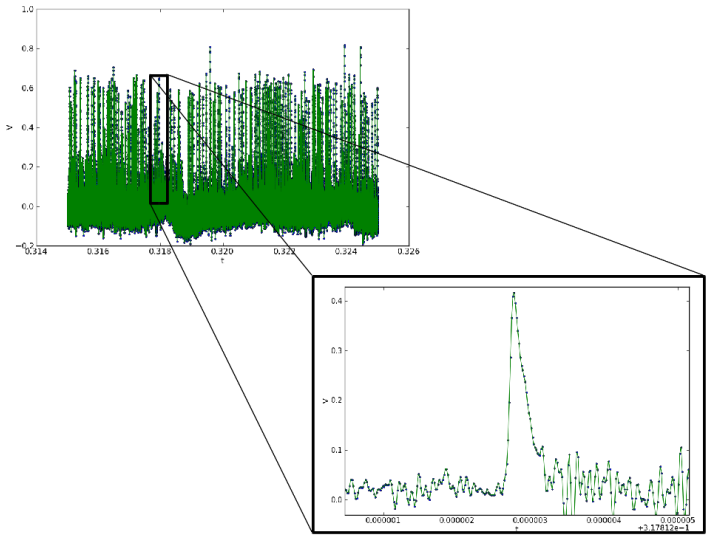

Figure 5: Example Peak

each point against its neighbors. The code checks through each voltage point in all individual time slices. Within a time slice, the variable $this$ is stored as the current voltage value and is compared to the local maximum and minimum voltages stored in mx and mn respectively. If $this$ is larger or smaller than mx or mn, it becomes the new local maximum or minimum. The script steps into the next logic check where it utilizes the threshold value previously mentioned. $this$ is compared to the local maximum mx minus the threshold value, $delta$, and if "True" the program will store the mx as a peak. The boolean value of $lookformax$ is then set to "True" so that the for loop repeats and continues to use the threshold logic check. Once a peak is found, the $lookformax$ is set to "False" and the script does another logic check for a "valley", lowest voltage point, to then reset the $lookformax$ boolean value to "True". The script also stores the valleys found in other logic checks, but wx_digiplot does not utilize them.

2.3 Peak Finding Script

```
mn, mx = Inf, -Inf
mnpos, mxpos = NaN, NaN
lookformax = True
for i in arange(len(v)):
        this = v[i]
        if this $>$ mx:
                mx = this
                mxpos = x[i]
```

```
                max_i = i
        if this < mn:
                mn = this
                mnpos = x[i]
                min_i = i
        if lookformax:
                if this < mx-delta:
                        maxtab_x.append(mxpos)
                        maxtab_y.append(mx)
                        maxtab_i.append(max_i)
                        mn = this
                        min_i = i
                        mnpos = x[i]
                        lookformax = False
        else:
                if this > mn+delta:
                        mintab_x.append(mnpos)
                        mintab_y.append(mn)
                        mintab_i.append(min_i)
                        mx = this
                        mxpos = x[i]
                        max_i = i
                        lookformax = True
return [maxtab_x,maxtab_y,maxtab_i],[mintab_x,mintab_y,mintab_i]
```

Particle rates are determined from the number of peaks corresponding to a proton event within the slice divided by the time width of the slice. Plots of the proton rates from each time slice as a function of time is related to the fusion rates during the plasma shot. Likewise, the neutron rate data are stored as rates versus time and will be compared to proton rates. Neutron data are obtained from Marco Cecconello's Neutron Camera.

In preparation for data analysis, a series of measurements were obtained at MAST outside of the tokamak during March of 2013 with an Americium-241 source. Americium-241 is a radioactive isotope that emits alpha (α) particles, helium nuclei of two protons and two neutrons. The purpose was to study data collection in the presence of electrical noise expected to originate from MAST. This data is separate from the data collected from MAST in August of 2013. Analysis revealed low electrical noise approximately around 100 millivolts. Rate plots generated with these data showed a contribution from electrical noise to alpha emission rates. Histograms of α peak heights showed a clear distinction between signal height distributions of electrical noise and alpha particles. Considering only the alpha particles, more accurate rate

plots are generated from that distribution.

A method of obtaining accurate rate data in spite of the presence of noise was developed along with handling particle signal pileups and superimposed particle-noise peak events. Proton peak pileups occur when two charged products are detected at the same time within the SSBD and consequently becomes categorized as one high voltage peak by the digitizer. Superimposed proton-noise peaks are the event when a particle is digitized directly on top a noise peak or valley making the height of the peak seemingly higher or lower. During the peak finding process this results in the erroneous categorization of peaks with an incorrect height. Although these events occur rarely, mitigation efforts are being developed to take them into account.

Categorizing each peak according to its height and sorting those values in a histogram shows the energy distribution of protons detected. The distribution of proton signals will ideally look like a Gaussian peak and should be distinguishable from any noise signal distribution. Histograms also display the existence of high voltage peaks that may possibly be proton peak pileups, high voltage noise, and superimposed proton peaks on noise peaks. If enough tritons are collected and/or distinguished from the electrical noise then a distribution of triton signals should appear as a noticeably smaller Gaussian peak in the histogram. The tritons show up as a smaller Gaussian peak because they are a lower energy than the protons.

3 Results

The data analyzed thus far has produced promising results. Most proton peaks are well above the electrical noise. Fortunately, some tritons are also distinguishable from the electrical noise as well but will require more intensive analysis. Preliminary data analysis shows that the time dependent neutron rates are consistent with the observed proton rates (Fig 8 & Fig 9). Initial histograms of different time slices show consistent signal distribution with prior alpha particle and noise histograms (Fig. 7). Occasionally, a triton signal distribution modeling a Gaussian peak is found within the histogram. The triton signal distribution becomes clear when the noise level is low enough. During data collection it was noted that channel 0 of the 4 channel DAQ occasionally became unable to detect proton signals, the reason for this behavior is at the moment unclear. There have been other observed irregular signal patterns that occur during the

end of the plasma shot for the other 3 channels that need to be addressed (Fig. 6).

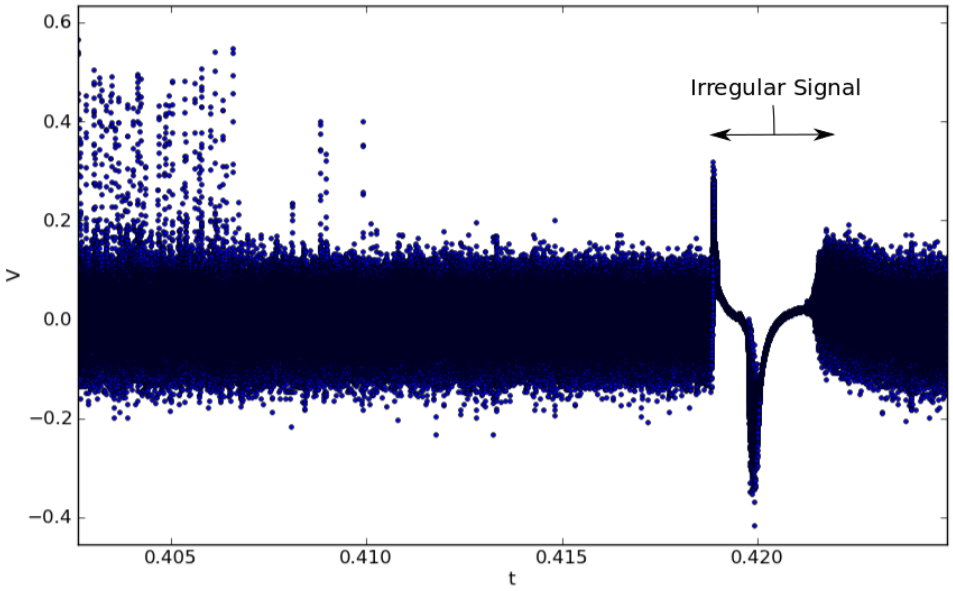

Figure 6: Strange signal pattern exhibited on a voltage vs time signal plot obtained from channel 1 of plasma shot 29809

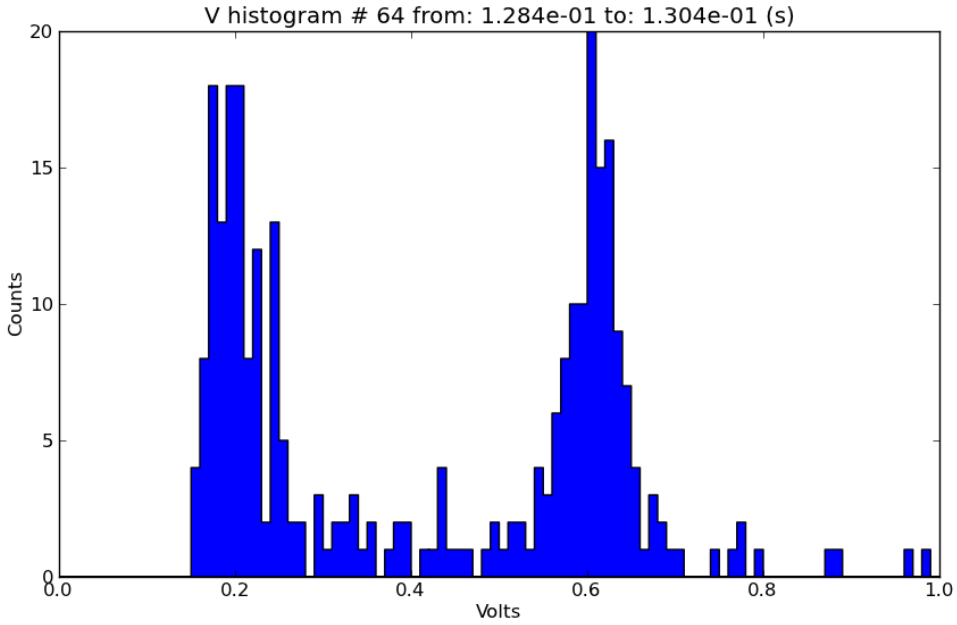

Figure 7: Voltage Histogram of a 3ms time slice from Channel 2 taken during plasma shot 29879. The rightmost peak represents the distribution of voltages for protons emitted during this shot.

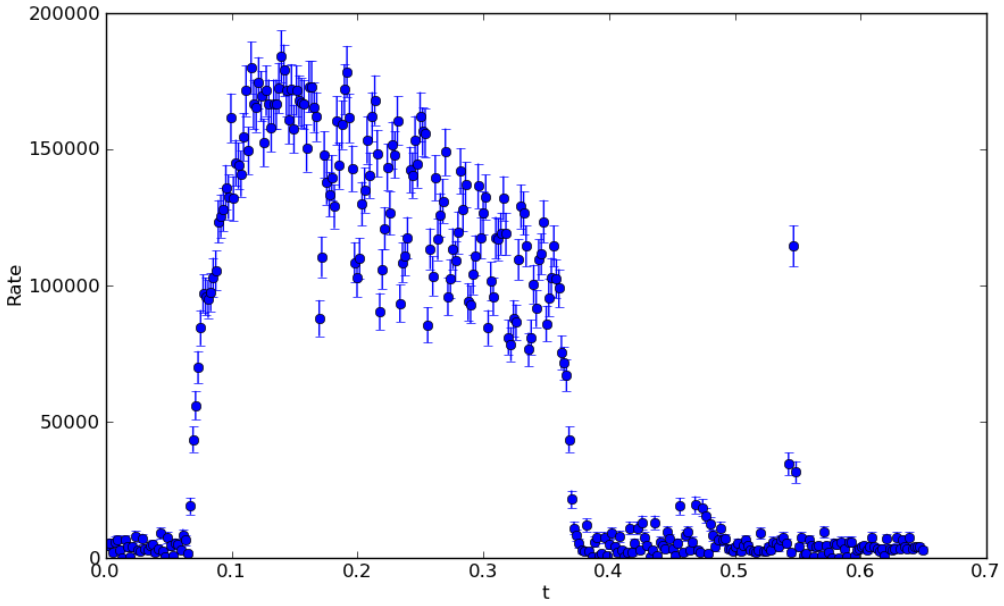

Figure 8: Proton rate plot of individual rates per 3 ms time slices for channel 2 of plasma shot 29879

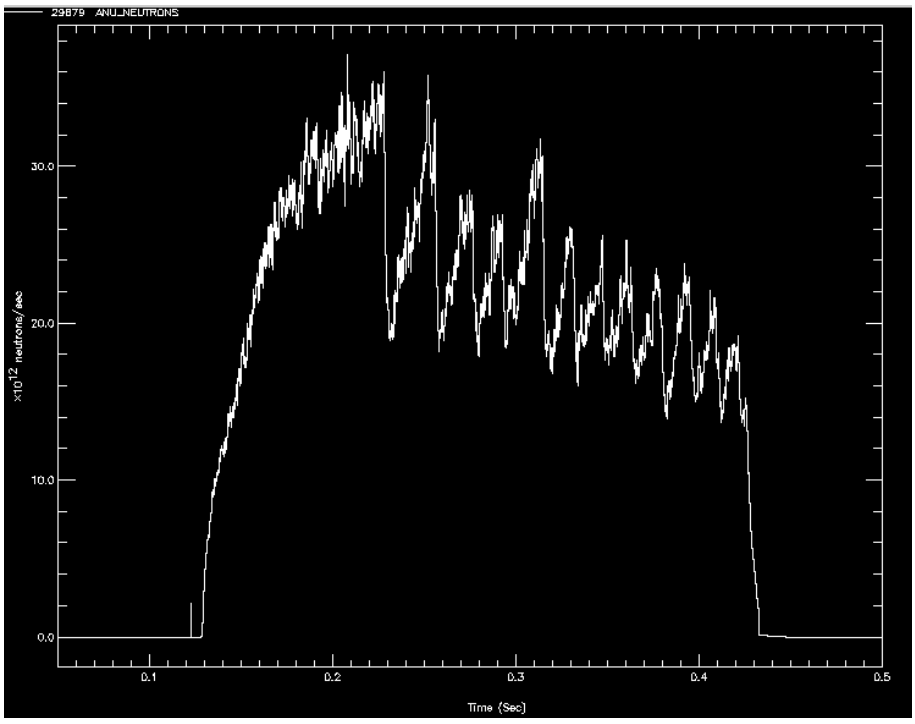

Figure 9: Neutron Rate Plot obtained from the Fission Chamber of plasma shot 29879

4 Discussion

Data collection has been completed on September 10, 2013. A full analysis of all plasma shots entails a thorough breakdown of proton rates, energies, and emission profiles during ”sawtooth” and ”fishbone” instabilities. Sawtooth instabilities develop when the core of the plasma radiates energy radially outward into the surface dropping in temperature. The surface of the plasma then rises in temperatures until an ejection of charged products exits the plasma. This instability shows up as sawtooth patterns in the data of charged particle rates versus time. Fishbone instabilities arise when the plasma wobbles at tens of thousands of vibrations per second, resulting in a surplus of ions and a deficiency quickly after. This shows up as spikes in the magnitude of the plasma's magnetic field. Finding the fusion reaction rates during these particular instabilities will help the understanding of their effects on the emissivity profile. Applying these completed results will lead to better diagnoses of plasmas as they are created in future tokamaks, and in future power generating fusion reactors.

5 Acknowledgements

I would like to extend my eternal gratitude to Dr. Werner Boeglin, and Ramona Valenzuela Perez for their guidance, thoughtfulness, and for showing me so much, especially that I am capable of so much if I believe in myself. I would also like to thank Douglass Darrow of the Princeton Plamsa Physics Laboratory for all of his help, hospitality, and stories. I would like to express my appreciation to my research colleagues Omar Leon, Adrianna Angulo, and Carlos Lopez for putting up with me and their endless assistance with this experiment. Scott Allan and Nigel of CCFE, thank you for aiding our project with your dedication and kindness. I wish to acknowledge Marco Cecconello of Uppsala University for making his data available to us and taking the time to share knowledge with me. I wish to thank the staff of CCFE for giving the FIU Experimental Plasma Physics group the opportunity to collect data. I would very much like to extend my sincerest gratefulness to my family for all of their inexhaustible continuous support. Lastly I would like to deeply thank the McNair Baccalaureate Fellowship Program at FIU for enabling me to embark on this truly memorable experience.

6 References

[1] J.A., Bittencourt. Fundamentals of Plasma Physics. 3rd Ed. New York, New York: Springer, 2004. Print.

[2] Friedberg, Jeffery. Plasma Physics and Fusion Energy. 1st Ed. Cambridge, United Kingdom: Cambridge University Press, 2007. Print.

[3] United Kingdom. United Kingdom Atomic Energy Authority. tokamak. Abingdon: Culham Centre for Fusion Energy, 2012. Web. ¡http://www.ccfe.ac.uk/Tokamak.asp&xgt;.

[4] United Kingdom. United Kingdom Atomic Energy Authority. MAST interactive diagram. Abingdon: Culham Centre for Fusion Energy, 2012. Web. ¡http://www.ccfe.ac.uk/MAST_diagram.asp&xgt;.

[5] Perez, Ramona Valenzuela. "A charged fusion product diagnostic for a spherical tokamak.." Florida International University Department of Physics Miami, Florida. (2012): n. page. Print.

[6] MAST plasma. 2012. Photograph. Culham Centre for Fusion Energy, Abingdon. Web. 28 Aug 2013. ¡http://www.ccfe.ac.uk/images_detail.aspx?id=9¿.

[7] tokamak met magneten 360 x 266 01.jpg [Web Photo]. Retrieved from http://www.energyresearch.nl/2/energy-options/nuclear-fusion/background/techniek/the-tokamak/

[8] Definition tokamak. (2013). Retrieved from http://www.merriam-webster.com/dictionary/tokamak

[9] (2013, 03 23). f1big.gif [Print Photo]. Retrieved from http://large.stanford.edu/courses/2013/ph241/kadribasic2/

[10] Cecconello, Marco, Dr. Neutron Measurements on MAST. Aug. 2013. Presentation. Culham, England.